Momentum Transport and Ion Heating From Reconnection in the Reversed Field Pinch

V. A. Svidzinski 1), F. Ebrahimi 1), V. V. Mirnov 1), S. C. Prager 1)

1) University of Wisconsin-Madison, Madison, Wisconsin and the Center for Magnetic Self-Organization in Laboratory and Astrophysical Plasmas, USA

e-mail contact of main author: vsvidzinski@wisc.edu

Abstract. Tearing instabilities and reconnection events in fusion plasmas can have enormous impact on the macroscopic behavior of the plasma. This is true in tokamaks, and is especially true in reversed field pinch plasmas, in which multiple tearing instabilities can be present. Two particularly large effects are the sudden transport of toroidal angular momentum and ion heating that occurs during a sawtooth crash in RFP experiments. During the crash, the radial profile of the toroidal rotation flattens and the ion temperature doubles, both in a time period of about $100\,\mu$s. Neither effect can be explained by classical processes. We report here analytic and computational results on mechanisms that can cause these effects through the action of tearing instabilities. The key findings are: (1) a single tearing mode can transport momentum through the Maxwell stress (the mean Lorentz force arising from tearing fluctuations), and the effect is greatly enhanced from the nonlinear interactions that accompany multiple tearing modes; (2) viscous damping of tearing modes can contribute significantly to ion heating, even in a plasma with low collisionality, given the strongly sheared flows that accompany tearing.

1. Momentum Transport

Magnetic fluctuations arising from MHD instabilities can cause momentum transport both in laboratory and astrophysical plasmas. In astrophysical plasmas, flow-driven instabilities are believed to transport momentum. Here, we investigate momentum transport from current-driven reconnection. Momentum transport is examined, both analytically and numerically, using the Maxwell stress associated with tearing instabilities. We study momentum transport from single tearing modes and transport from multiple tearing modes. We find that a single tearing mode can transport momentum, but that transport is substantially enhanced in the presence of multiple modes due to nonlinear mode coupling.

Tearing fluctuations are believed to play an important role in sustaining the reversed field pinch (RFP) configuration. It is also believed that the momentum transport observed experimentally is related to the nonlinear torques arising from the tearing fluctuations. Large toroidal flow (about a few percent of V_A) has been observed in the RFP. Experimental measurements have shown a rapid momentum transport as the toroidal flow profile flattens during a reconnection event [1]. Momentum transport is faster than can be explained by collisional viscosity. The Maxwell and Reynolds stresses arising from tearing instabilities are believed to be the leading explanation for momentum transport. Previous theoretical studies have investigated the role of nonlinear interaction of tearing modes on plasma momentum in the RFP [2, 3]. The internal electromagnetic torques from three wave coupling and the torques from external field errors have been calculated via quasilinear theory using ideal MHD eigenfunctions. It has been shown that the electromagnetic torque at each resonant surface is nonlinearly related to the amplitudes of the magnetic

field perturbations of the three tearing modes. These studies have been based on the ideal MHD equations. Here, in the presence of mean flow, we evaluate the torques (Maxwell and Reynolds) from a single tearing mode by including the inner layer dynamics in the cylindrical geometry [4]. We employ nonlinear, resistive MHD computation to evaluate the important effect of nonlinear coupling of multiple tearing modes on the torques.

To investigate momentum transport from single tearing mode in the nonlinear state and the role of nonlinear mode coupling on momentum transport, nonlinear, 3D, resistive MHD code, DEBS, [5] is employed

$$\begin{aligned} \frac{\partial \overline{A}}{\partial t} &= S\overline{V}\times\overline{B} - \eta\overline{J} \\ \rho\frac{\partial \overline{V}}{\partial t} &= -S\rho\overline{V}.\nabla\overline{V} + S\overline{J}\times\overline{B} + P_m\nabla^2\overline{V} + \mathbf{F}(r) \\ \overline{B} &= \nabla\times\overline{A} \\ \overline{J} &= \nabla\times\overline{B} \end{aligned}$$

where $S = \frac{\tau_R}{\tau_A}$ (Lundquist number) , $P_m = \frac{\tau_R}{\tau_{vis}}$ (magnetic Prandtl number = viscosity / resistivity). With an axial ad-hoc momentum source term $\mathbf{F}$(r) added to the momentum equation.

First, we investigate momentum transport from a single tearing mode. We perform nonlinear evolution of a tearing mode in the presence of axial mean flow. We employ DEBS code for the single helicity computation in the presence of an ad-hoc momentum source. Force free equilibrium is used for a core tearing mode, m=1, $k_z = 2$. The Lorentz force, $< \widetilde{J}\times\widetilde{B} >_z$ arising from the Maxwell stress , during the linear growth phase is shown in *FIG. 1.* As is seen the stress term is localized around the resonant surface. Because of the nonzero viscosity in the computation, the fluid stress term is smaller than the Lorentz term. During the nonlinear phase, the flow profile is flattened by the Lorentz force around the resonant surface. Because $\widetilde{B}_r$ and $\widetilde{B}_z$ are out of phase, in the absence of flow, the Lorentz force for a single mode is zero. In the presence of the flow, the nonzero contribution arises from the phase between $\widetilde{B}_r$ and $\widetilde{B}_z$ around the resonant surface as shown in *FIG. 2.* We have also obtained the Lorentz term from a single tearing mode in the outer region (ideal region). It is found that the force is directly related to the tearing growth rate and the flow shear. Using analytical quasilinear calculations, we have also shown that the major contribution of the nonzero torques arises from the inner layer solutions which agrees with the single mode computations.

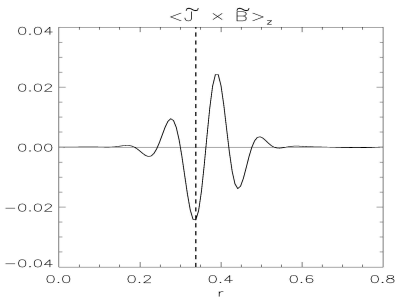

FIG. 1. Axial Maxwell stress term $< \widetilde{J}\times\widetilde{B} >_z$*, from single helicity computation,* $S = 10^5$, $Pm = 1$.

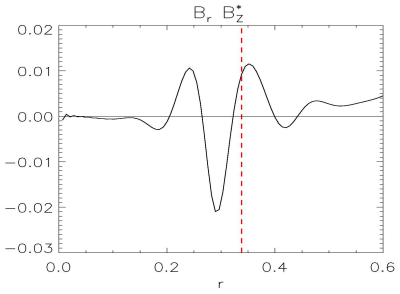

FIG. 2. Radial structure of $\cos(\delta)$*, where* δ *is the phase between* $\widetilde{B}_r$ *and* $\widetilde{B}_z^*$ *during the linear phase of single helicity computation (*$< \widetilde{J} \times \widetilde{B} >= \frac{1}{r}\left[r|\widetilde{B}_z||\widetilde{B}_r|\cos(\delta)\right]'$*).*

We perform multiple helicity computations at Lundquist number $S = 10^4$ with the ad-hoc momentum source. The correlation of the relaxation events with the flow profile can be investigated in these computations. The simulations are started to build the standard RFP configuration at aspect ratio R/a=1.66, and Prandtl number $P_m = 10$. After reaching a quasi-stationary RFP state, the ad-hoc force is switched on at the time $t/\tau_R = 0.3$ with a radial profile F(r)=const. Figure 3 shows the time history of the total magnetic fluctuations. The axial flow profile would evolve to be parabolic in radius in the absence of fluctuation-induced forces. After the force is applied the axial flow builds, saturating at $V_z = 0.04 V_A$. Total fluctuation-induced Lorentz force $< \tilde{J} \times \tilde{B} >_z$ at times t_1 and t_2 are also shown in *FIG. 4*. The Lorentz force is larger at time t_2 and changes sign in the core. The flow profile is flattened in the plasma core at time t_2. The flattening arises from the total Lorentz force from tearing fluctuations (*FIG. 4*). To clarify the effect of nonlinear mode coupling, we have also performed nonlinear computations in which m=0 mode is removed. It is found that momentum transport is greatly reduced.

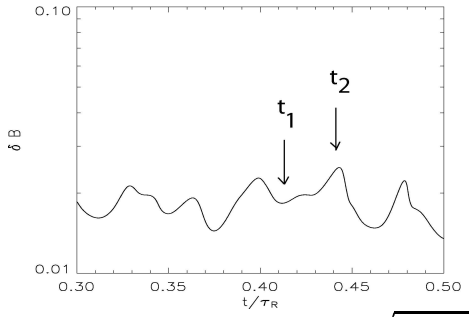

FIG. 3. Total volume integrated magnetic fluctuation $\sqrt{1/2 \int B_r^2 dv}$ *vs. time (*$S = 10^4$*).*

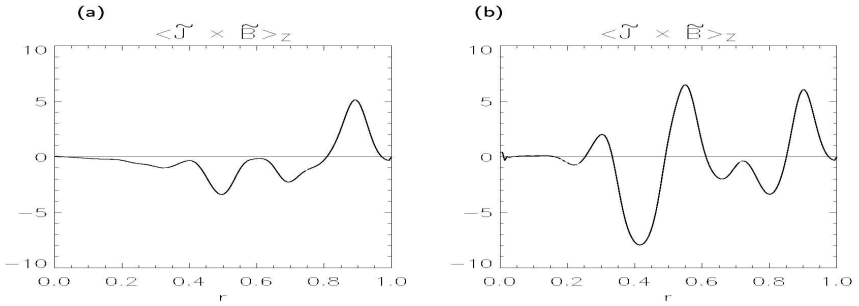

FIG. 4. Radial structure of (a) total $< \tilde{J} \times \tilde{B} >_z$ *term at* $t_1 = 0.41$ *and (b) at* $t_2 = 0.44$ *from multiple helicity computation(summed over all n and m mode numbers).*

In summary, we have shown that the stress terms arising form tearing instabilities can cause momentum transport in the RFP. Using quasilinear theory and nonlinear single mode computation, we have established that a single tearing mode can transport momentum in the presence of mean flow. Multiple helicity computations show stronger momentum transport because of the nonlinear coupling.

2. Ion Heating

Strong ion heating is observed in the reversed field pinch. During a sawtooth crash in the Madison Symmetric Torus RFP the ion temperature can spontaneously double in $\sim 100\,\mu$s. It is also observed that high Z impurities are heated stronger than bulk ions. Figure 5 shows measured dependence of impurity temperature versus time relative to sawtooth crash.

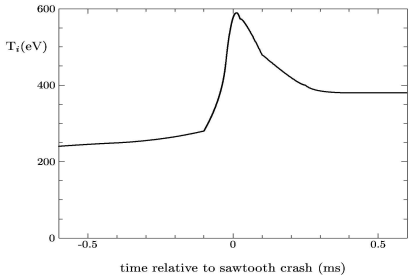

FIG. 5. Impurity temperature vs. time.

The heating may arise from tearing instabilities due to irreversible transfer of kinetic flow energy into heat caused by ion-ion collisions (viscosity). At the sawtooth crash numerous tearing modes are unstable. A tearing mode is connected with a resonant surface in plasma for which safety factor $q(r) = \frac{rB_\phi(r)}{RB_\theta(r)} = m/n$. The component of the wave vector of the tearing mode parallel to the equilibrium magnetic field is zero at the resonance. Typical RFP q-profile with the location of tearing resonances is shown in *FIG. 6.* Radial locations of resonant surfaces of different tearing modes are spreaded along minor radius. Velocity perturbation in the mode is localized near its resonant surface. Thus, ions are heated near the resonant surface of each mode. Individual contributions of each mode lead to the ion heating in the plasma volume.

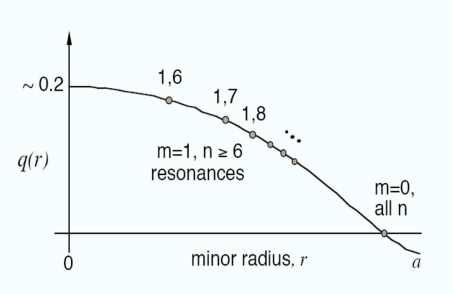

FIG. 6. RFP q-profile.

Components of perturbations of magnetic field and velocity in a linear tearing eigenmode with wave numbers $m = 1$, $n = 6$ are shown in *FIG. 7.* The profiles are calculated

in cylindrical geometry. A force free magnetic equilibrium is assumed with $J_\parallel/B = 4[1-(r/a)^2]$; plasma pressure is uniform with $\beta = 0.2$. Component v_η on this plot is perpendicular to radial and parallel components. Perturbation of magnetic field is distributed over minor radius while velocity perturbation is localized near the resonance surface, its width depends on plasma resistivity (here, the Lundquist number is $S = 10^5$).

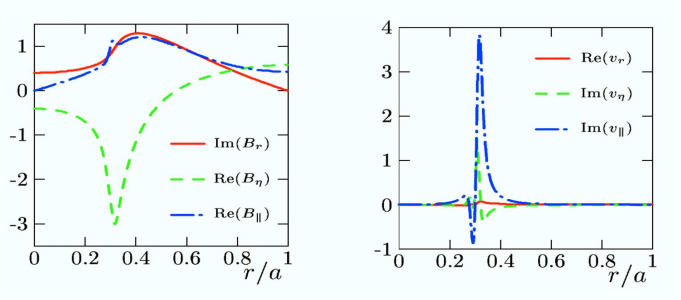

FIG. 7. Field components in tearing eigenmode.

Velocity profile in the tearing mode is strongly sheared in radial direction. Thus, viscous heating can be sizable. The major contributions to the ion heating are

$$Q_{vis} = \eta_\perp \left(\frac{\partial v_\eta}{\partial r}\right)^2 + \eta_\parallel \left(\frac{\partial v_\parallel}{\partial l_\parallel}\right)^2 + \eta_\perp \left(\frac{\partial v_\parallel}{\partial r}\right)^2 . \qquad (1)$$

The first and the third term correspond to viscous heating due to radial shear of v_η and $v_\parallel$. The second term is heating due to parallel gradient of $v_\parallel$ in the vicinity of the resonance (it is zero at the resonance). For estimate of ion temperature increase we assume that each mode heats plasma in a small volume in which its velocity perturbations are localized.

In our model the plasma parameters are as follows. $B = 1.5 \times 10^{-1}\,\mathrm{T}$, $T = 200\,\mathrm{eV}$, $n_e = 10^{19}\,\mathrm{m}^{-3}$, bulk ions with $Z = 1$ and $m_i/m_p = 2$, single species impurity with $Z = 6$, $m_Z/m_p = 12$. The ion and impurity densities $n_i = 0.64\,ne$, $n_Z = 0.06\,n_e$. For these parameters, $v_{Ti}/v_A = 0.11$, $v_{TZ}/v_A = 0.044$, $\rho_{Li} = 1.4\,\mathrm{cm}$, $\rho_{LZ} = 0.56\,\mathrm{cm}$.

For the estimate of ion heating one needs to know the value of velocity amplitude and it spatial profile. In the experiment the amplitude of magnetic field perturbation at the crash (with the poloidal wave numbers $m = 0$ or $m = 1$) is of the order of 2% of equilibrium field. Because there is a defined ratio between magnetic field and velocity amplitudes in the linear eigenmode, one can deduce the value of velocity amplitude corresponding to such perturbation of magnetic field. In reality tearing modes evolve nonlinearly and more accurate estimates based on solution of nonlinear resistive MHD equations are required. The difficulty in nonlinear modeling is that typical simulation in these parameter range requires strong artificially introduced viscosity (several orders of magnitude higher than realistic one). This viscosity makes 3-D simulations feasible but it limits the radial width and diminishes amplitudes of small scale velocity perturbations. Such limitations are crucial for the heating estimates since the heating rate is quadratic in velocity amplitude and radial wave number. We implemented an algorithm for solving the equations without the introduction of artificially strong viscosity. Because the simulation requires more computing power we implemented it in 2-D plane geometry.

We solve resistive MHD equations in xy plane. There are conducting walls at $x = 0$ and $x = L_x$. The solutions are periodic in y coordinate with the period L_y and do not depend on z. There is an RFP-like force free equilibrium with magnetic field components B_y and B_z. The equilibrium is chosen to be tearing unstable with the linear growth rate of the eigenmode comparable with the experimental value. Fourier transform of equations in x and y coordinates is made. Time evolution of the Fourier coefficients is carried out numerically by an explicit method. In this approach small or zero viscosity in the model does not influence numerical stability.

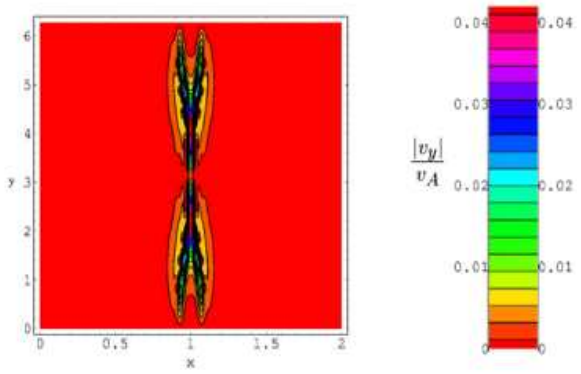

FIG. 8. Profile of $|v_y|/v_A$ in xy plane.

Figure 8 shows profile of $|v_y|/v_A$ in the xy plane at the moment of time when the amplitude of magnetic perturbation reached 2% of equilibrium magnetic field. At this moment of time a spectrum of Fourier harmonics corresponding to x and y coordinates is excited. The maximum magnitude of v_y is comparable to the thermal velocity of impurity. The velocity profile is strongly localized near the resonance $x = 0$, its width is of the order of ion gyroradius. In spite of the nonlinear time evolution, the result is similar to the estimates based on the linear eigenmode.

We estimate the ion heating assuming that spatial and time dependence of velocity is a specified function. For the considered plasma parameters collision times, estimated as

$$\nu_{\alpha\beta} = \frac{4\pi e_\alpha^2 e_\beta^2 L_c n_\beta}{m_\alpha^2 v_{T\alpha}^3},$$

are $\tau_{ZZ} = 2.5\,\mu$sec, $\tau_{ii} = 123\,\mu$sec, $\tau_{Zi} = 8.3\,\mu$sec, $\tau_{iZ} = 37\,\mu$sec. The duration of the sawtooth crash is $100\,\mu$sec. On this time scale the impurities are strongly collisional while the bulk ion collision time is of the order of heating time. The scale of perpendicular variation of velocity is comparable to the ion gyroradius. Thus an accurate modeling of collision operator is required for the estimate of the heating rate.

Contribution to ion heating from $\eta_\perp \left(\frac{\partial v_\eta}{\partial r}\right)^2$ is estimated as follows. Electric field $E_x(t,x) = E \sin\left(\frac{\pi t}{100\,\mu sec}\right) \sin\left(\frac{\pi x}{L}\right)$ is applied in the magnetized plasma with $\boldsymbol{B} = B_0 \boldsymbol{e_z}$. During the time evolution plasma is uniform in y and z directions. Such electric field models perpendicular electric field in the tearing mode, it drives $\boldsymbol{E} \times \boldsymbol{B}$ flow which is sheared in x

direction. We solve kinetic equation with Landau collision operator for the ion distribution function $f(t, x, v_x, v_y, v_z)$ which is assumed to be periodic in x coordinate with the period $2L$.

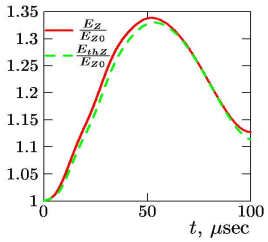

FIG. 9. Volume averaged kinetic and thermal energy of impurity vs. time.

Time dependence of kinetic energy and thermal energy of impurity averaged over $-L < x < L$ is shown in *FIG. 9.* The calculation is made for $E = 10^4$ V/m and $L/\rho_{LZ} = 3.6$. Dependence of velocity components of impurity versus x/ρ_{LZ} is shown in *FIG. 10* at the moment of time $t = 50\mu$ sec. v_y component follows $\boldsymbol{E}\times\boldsymbol{B}$ profile modified by finite Larmor radius effect. There is a significant perturbation of the impurity density with the maxima at $x = -L$ and $x = L$ and minimum at $x = 0$. The distribution functions of impurity at cross-section $v_z = 0$ and two spatial locations are presented in *FIG. 11.* Because of the strong collisionality the distribution functions are shifted Maxwellians. Kinetic energy and thermal energy at $t = 50\mu$sec versus spatial scale L is shown in *FIG. 12.* For smaller L/ρ_{LZ} the flow is suppressed due to a large Larmor radius and the heating is diminished. For large L/ρ_{LZ} the flow shear and the heating is reduced. Thus there is an optimal scale L for which the heating is most effective.

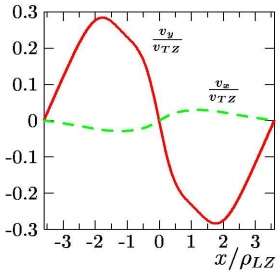

FIG. 10. Velocity components vs. x/ρ_{LZ}.

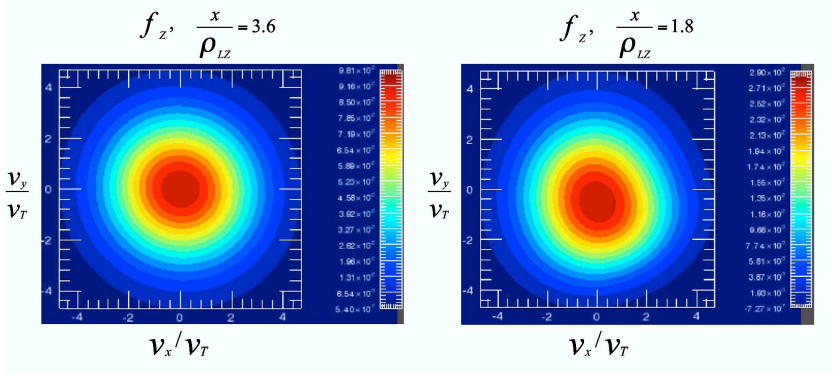

FIG. 11. Impurity distribution functions.

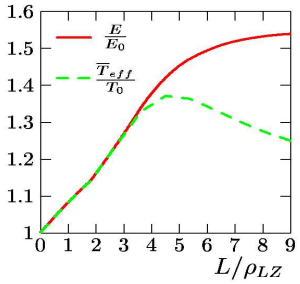

FIG. 12. Volume averaged kinetic and thermal energy of impurity vs. L.

Similar calculations where carried out for bulk ions. Results show that impurities are heated stronger than bulk ions due to several reasons. Due to high Z impurities respond stronger on given electric field than bulk ions. Their collision rates are higher. Drift velocity of impurity relative to its thermal velocity is larger than that of bulk ions.

Similar models are developed for the estimate of contribution to the ion heating from $\eta_{\parallel}\left(\frac{\partial v_{\parallel}}{\partial l_{\parallel}}\right)^2$ and $\eta_{\perp}\left(\frac{\partial v_{\parallel}}{\partial r}\right)^2$. In the models the flows are driven by applied electric field and the kinetic equation with Landau collision operator is solved numerically for the estimate of ion temperature increase. The results are similar to the previous case. Heating of impurities is stronger than the heating of bulk ions. When the three contributions to the ion heating of Eq. (1) are combined, it results in a strong heating of impurities and qualitatively explains the experimental result. The bulk ion heating estimated from these models is still smaller than the one observed in the experiment. Estimates show, however, that the direct heat transport from impurities to bulk ions due to ion-impurity collisions is sizable and could explain the heating of bulk ions.

References

[1] HANSEN, A. K., et al. PRL **85**, 3408 (2000)

[2] FITZPATRICK, R., Phys. Plasmas (6), 1168 (1999)

[3] HEGNA, C. C., Phys. Plasmas **3**, 4646 (1996)

[4] COPPI, B., GREENE, J. M., JOHNSON, J. L., Nucl. Fusion, **6**, 101, 1966

[5] SCHNACK, D. D., BARNES, D. C., MIKIC, Z., HARNED, D. S., and CARAMANA, E. J., J. Comput. Phys. **70**,330 (1987)